Cell Stress and Chaperones (2022) 27:633–643
https://doi.org/10.1007/s12192-022-01301-0

ORIGINAL ARTICLE

Endoplasmic reticulum stress and unfolded protein accumulation correlate to seizure recurrence in focal cortical dysplasia patients

Kishore Madhamanchi[1] · Pradeep Madhamanchi[1,2] · Sita Jayalakshmi[3] · Manas Panigrahi[3] · Anuja Patil[3] · Prakash Babu Phanithi[1]

Received: 13 June 2022 / Revised: 28 September 2022 / Accepted: 28 September 2022 / Published online: 18 October 2022

Abstract

Epileptic seizures occur due to an imbalance between excitatory and inhibitory neurosignals. The excitotoxic insults promote the accumulation of reactive oxygen species (ROS), unfolded proteins (UFP) aggregation, and sometimes even cell death. The epileptic brain samples in our study showed significant changes in the quantity of UFP accumulation. This part explored the efficiency of ER stress and autophagy responses at neutralizing the UFP using resected epileptic brain tissue samples. Meanwhile, we regularly observed these patients' post-surgical clinical data to find the recurrence of seizures. According to International League against Epilepsy (ILAE) suggestions, we classified the patients ($n=26$) as class 1 (completely seizure-free), class 2 (less frequent seizures or auras), and class 3 (auras with <3 seizures per year). The classification helped us understand the reason for variations in the UFP accumulation in patient samples. We have observed the protein levels of ER chaperone, glucose-regulated protein 78 kDa (GRP78/BiP), inositol-requiring enzyme 1α (IRE1α), X box-binding protein 1 s (XBP1s), eukaryotic translation initiation factor 2α (peIF2α), C/EBP homologous protein (CHOP), NADPH oxidase (NOX2), and autophagy proteins like BECLIN1, ATG 7, 12, 5, 16, p62, and LC3. Our results suggested that ER stress response limitation may contribute to seizure recurrence in epilepsy patients, particularly in classes 2 and 3. In addition, we have observed significant upregulation of ER stress-dependent apoptosis initiation factor CHOP in these patients. These results indicate that understanding the ER stress response pattern infers the possibility of post-surgical outcomes in focal cortical dysplasia (FCD) patients.

Keywords Focal cortical dysplasia (FCD) · Endoplasmic reticulum stress · Unfolded protein response (UPR) · Oxidative stress · Autophagy · Clinical outcome

Introduction

In both the pediatric and adult populations, focal cortical dysplasia (FCD) is a major cause of drug-resistant epilepsy (Kabat and Król 2012). FCD occurs due to the malformation of the cortex during brain development. Amongst its subtypes, type I has disruption of intracortical lamination and columnar organization. Cortical dyslamination and dysmorphic neurons characterize type IIa, while balloon cells describe type IIb (Palmini et al. 2004; Krsek et al. 2008; Kim and Choi 2019). Both FCD types I and II are associated with intractable epilepsy. Most patients with FCD show recurrent seizures even after using antiepileptic drugs (Kwan et al. 2010). One-third of the patients affected by epilepsy respond poorly to contemporary antiepileptic medicines (Liu et al. 2019). As a chronic neurological disorder, epilepsy often contributes to neurodegeneration due to disturbance in the endoplasmic reticulum (ER) homeostasis. ER stress is triggered by various intracellular and extracellular stimuli, such as reducing disulfide bonds, ER calcium reserves, impairment of protein transport to the Golgi, increased protein load, and absence of ER-associated protein degradation (Kadowaki and Nishitoh 2013). Nearly 30% of newly formed proteins in the ER degrade due to folding defects (Schubert

✉ Prakash Babu Phanithi
prakash@uohyd.ac.in

[1] Department of Biotechnology and Bioinformatics, School of Life Sciences, University of Hyderabad, Hyderabad, Telangana 500046, India

[2] Govt. Degree College for Men, Srikakulam District, Andhra Pradesh 532001, India

[3] Department of Neurology, Krishna Institute of Medical Sciences (KIMS), Secunderabad, Telangana, India

et al. 2000). Any perturbations in the ER function led to the accumulation of unfolded proteins and initiate unfolded protein response (UPR) to maintain ER homeostasis (Wu and Kaufman 2006; Bravo et al. 2013).

ER-dependent UPR is initiated by the release of ER chaperone (BiP/GRP78) from three proximal ER stress sensors: PERK (protein kinase R-like ER kinase), IRE1 (Inositol-requiring enzyme 1), and ATF6 (activating transcription factor 6) (Kim et al. 2008). GRP78 binds to UFP and assists in folding. The kinase domain of PERK successively phosphorylates eIF2α (Harding et al. 1999) and attenuates protein translation to ease the ER protein load. ATF4, a transcription factor not affected by peIF2α, turns on genes required for protein folding and autophagy (B'chir et al. 2013). Autophosphorylation of IRE1α splices XBP1 (X-box binding protein1) mRNA, leading to the generation of a potent transcriptional activator that induces ER stress-responsive genes. All three major arms of ER stress signaling pathway, i.e., PERK, IRE1, and ATF6 converge on the elements in the CCAAT enhancer-binding protein (C/EBP) homologous (CHOP) promoter region to induce the expression of pro-apoptotic molecule CHOP/GADD153 (Zinszner et al. 1998; Oyadomari et al. 2002; Oyadomari and Mori 2004) during chronic ER stress conditions (Hu et al. 2019). XBP1s axis also regulates Beclin1 and microtubule-associated protein1 light chain-3B (LC3B) to activate the autophagy mechanism. NADPH oxidase 2 (Nox2) enhances ROS production and oxidative stress (Pal et al. 2014; Henríquez-Olguin et al. 2019). Accumulation of ROS can also inhibit the autophagy flux (Pal et al. 2014, 2016).

ER stress contributes to neuronal damage during epilepsy-induced seizures (Zhu et al. 2017). Chronic ER stress can alter neuronal morphology and potentially enhances apoptotic signaling in epilepsy patients (Rao et al. 2004; Sokka et al. 2007; Kim et al. 2008). Further research into the relationship between ER stress and seizure severity is required to establish a link between the ER stress response and post-surgical seizure outcomes in patients.

Methods

Sample collection and ethical guidelines

We collected the epileptic brain samples from the hospital immediately after the surgery. An experienced epilepsy pathologist classified the patients as FCD type I, IIA, and IIB at Krishna Institute of Medical Science (KIMS). The written informed consent was obtained from patients or their relatives. The KIMS Foundation and Research Centre and KIMS Ethical Committee, Secunderabad, India, approved the study protocol, which followed the Institutional Ethical Committee guidelines. All the subjects were completely anonymized. For future studies, the epilepsy samples were collected immediately and stored at − 80 °C. The human brain tissue repository at the National Institute of Mental Health and Neuro-Science (NIMHANS), Bangalore, India, provided the autopsied control brain samples for this study. The control brain samples were not suitable for immunofluorescence assay. Hence, we used these control brains only for western blot assays.

Hematoxylin and eosin staining

This is the most useful technique in histopathology; two kinds of dyes (Hematoxylin & Eosin) are used to stain different parts of the tissues differentially. Hematoxylin is a basic dye that binds to nucleic acids and ribosomes and imparts blue-purple color, whereas eosin is an acidic dye that binds to basic elements like cytoplasm and collagen and imparts pink/orange/red color. In our study, some part of resected epilepsy brain tissue was rinsed with phosphate-buffered saline (PBS) and stored at room temperature by soaking in a 4% formalin solution after surgery. 24 h later, tissues were rinsed with water and dehydrated with different grades of ethanol (70%, 80%, 90%, and 100%) and embedded in paraffin wax after 100% ethanol, xylene (1:1) treatment. 5-µm-thick sections were sliced from paraffin wax-embedded tissue blocks. The tissue slices were placed on a glass slide, dewaxed with xylene, rehydration with ethanol (100%, 90%, 80%, 70%), and rinsed with water, then dried. The tissues were stained with hematoxylin for 3–5 min and then washed under tap water. The sections were dipped in 1% acid alcohol (1% HCl, 70% ethanol) for a few seconds, followed by a rinse with water. Dip the slides in ammonia water until the sections become blue and wash with water. Stain the sections with 1% Eosin Y for 10 min, wash them in tap water, and dehydrated them with 90% and 100% ethanol. After dehydration, the slides were kept in xylene for clearing, then washed with water. Finally, the tissue sections were covered with coverslips using mounting media and allowed for curing overnight. The images were captured using an Olympus microscope.

Thioflavin T fluorescence assay

Thioflavin T (T3516, Sigma-Aldrich), a benzothiazole salt, is widely used for protein aggregate quantification (Beriault and Werstuck 2013). Thioflavin T binds to unfolded protein (UFP) aggregates, like β-sheets, and gives enhanced fluorescence. 100 µg of protein was added to Milli Q water and made up the volume to 50 µl in a 96-well plate. 2 µl of freshly prepared 0.5 mM Thioflavin T stock solution was added to make the final working concentration of 20 µM. After 30 min of incubation, the fluorescence intensity of each sample was measured using a Tecan spectrofluorometer

infinite® 200 PRO. The excitation and emission wavelengths of the microplate reader were set at 440 nm and 490 nm, respectively.

Tissue lysate and western blot analyses

The radioimmunoprecipitation assay buffer was used to prepare the whole-cell lysate in the Dounce homogenizer at 4 °C. Protease inhibitor (Sigma-Aldrich, cat: no. P8340) and phosphatase inhibitor (Sigma-Aldrich, cat: no. P5726) were added to 100 mg of tissue sample before adding RIPA buffer. After that, tissue lysate was centrifuged at 14,000 rpm for about 15 min at 4 °C. The supernatant was separated, and the proteins were quantified using the Bradford reagent. (B6916 Sigma-Aldrich). 45 µg of protein sample suspended in a 6 × sample buffer (20% glycerol, 4% Sodium dodecyl sulfate (SDS), 0.125 M Tris, pH 6.8, 0.02 M dithiothreitol, 0.02% bromophenol blue). After that, the proteins were resolved by the SDS-PAGE. The gel was transferred to the nitrocellulose membrane (Protran Amersham GE) overnight at 4 °C using the Towbin buffer (Tris base, Glycine, Methanol, pH 8.3) at 25 V. Tris-buffered saline (TBS) and TBS containing 0.05% Tween 20 (TBST) were used to wash the membrane. The nitrocellulose membrane was blocked with non-fat skimmed milk powder (Sigma- Aldrich: M7409) in TBST to reduce non-specific binding. At 4 °C, these blots were incubated with primary antibodies overnight. The antibodies used for this study were BiP (Cell signaling technology [CST]-3177), p-IRE1α (Novus Biological [NBP]100-2323SS), CHOP (CST-2895), XBP1 (NBP2-20917), p-eIF2α (CST-3398), Beclin (CST-3495) P62 (CST-39749 s), NOX2 (NBP2-41291), LC3B (CST-3868), ATG16L (CST-8089), ATG12 + 5 (MA5-27801), and ATG7 (CST-2631) diluted to 1:1000 in TBST buffer overnight at 4 °C. After subsequent washing with TBS and TBST, the blots were probed with secondary antibodies (1:15,000 dilutions), anti-rabbit (CST-7074P2), and anti-mouse IgG (CST-G21040) conjugated to HRP for one hour at room temperature. The blots were developed using a chemiluminescence reagent (ClarityTM Western ECL substrate 1705060) and a Bio-Rad (Bio-Rad, USA) molecular imager.

Double immunofluorescence assay

5-µm-thick paraffin-embedded tissue sections were deparaffinized, hydrated with xylene, 100%, and 95% ethanol, respectively, and washed with distilled water. Antigen was retrieved using boiled citrate buffer for 15 min (10 mM citrate buffer pH 6.0) and allowed to cool. The sections were covered with blocking buffer (5% normal goat serum, CST-5425, 1% BSA in 1 × PBS supplied with 0.3% Triton X-100) and kept in a humid chamber for 1 h at room temperature. The blocking buffer was removed from the tissue sections after incubation. The primary antibody cocktail was added and then incubated at 4 °C for 16 h to examine the neuronal expression of XBP1s (CST 12782) rabbit monoclonal antibody and NeuN (MAB377B) mouse antibody at 1:100 dilutions in antibody dilution buffer (CST-12378). The sections were washed with 1 × PBS and incubated with fluorochrome-conjugated secondary antibodies, anti-rabbit IgG conjugated with Alexa fluor® 488 (CST-4412S), and anti-mouse IgG conjugated with Alexa fluor® 555 (CST-4409S) diluted in antibody dilution buffer for 1–2 h at room temperature in the dark. Sections were washed in 1 × PBS and mounted with the Prolong® Gold anti-fade reagent with DAPI (CST-8961S). The ZEN Blue software was used for image acquisition with Carl Zeiss LSM 710, and the Image J software was used to quantify fluorescent intensities.

Data analysis

Statistical analysis among groups was performed using one-way analysis of variance (ANOVA) using the Newman-Keuls method for post hoc analysis. Data were reported as mean ± SEM. The P-value < 0.05 was considered statistically significant and was determined using the Sigma Plot 2000 software for Windows.

Results

Neuropathological analysis of tissue samples

Figure 1 depicts cellular morphologies of FCD type I, FCD type IIa, and FCD type IIb by hematoxylin and eosin staining of samples obtained from the FCD patients. The postoperative follow-up study was performed on patients to understand the possible seizure outcome according to the International League Against Epilepsy (ILAE) (Wieser et al. 2001). Table 1 represents the FCD patients' ($n = 26$) clinical characteristics, postoperative follow-up data, and seizure outcomes. The follow-up data of these FCD patients suggests that ten patients belong to the ILAE class1 (38.46%), nine patients belong to the ILAE class 2 (34.69%), and seven patients (26.92%) belong to the ILAE class 3. Table 2 represents the control sample ($n = 3$) data obtained from NIMHANS, which include age, gender, cause of death, the time interval between death and postmortem, neuropathology, disease condition, and infections; post-operative tissue samples were collected and stored at the NIMHANS brain bank using a standardized protocol.

Accumulation of unfolded proteins

The ER is critical for appropriately folding the proteins or enzymes and regulating many signaling pathways (Schwarz

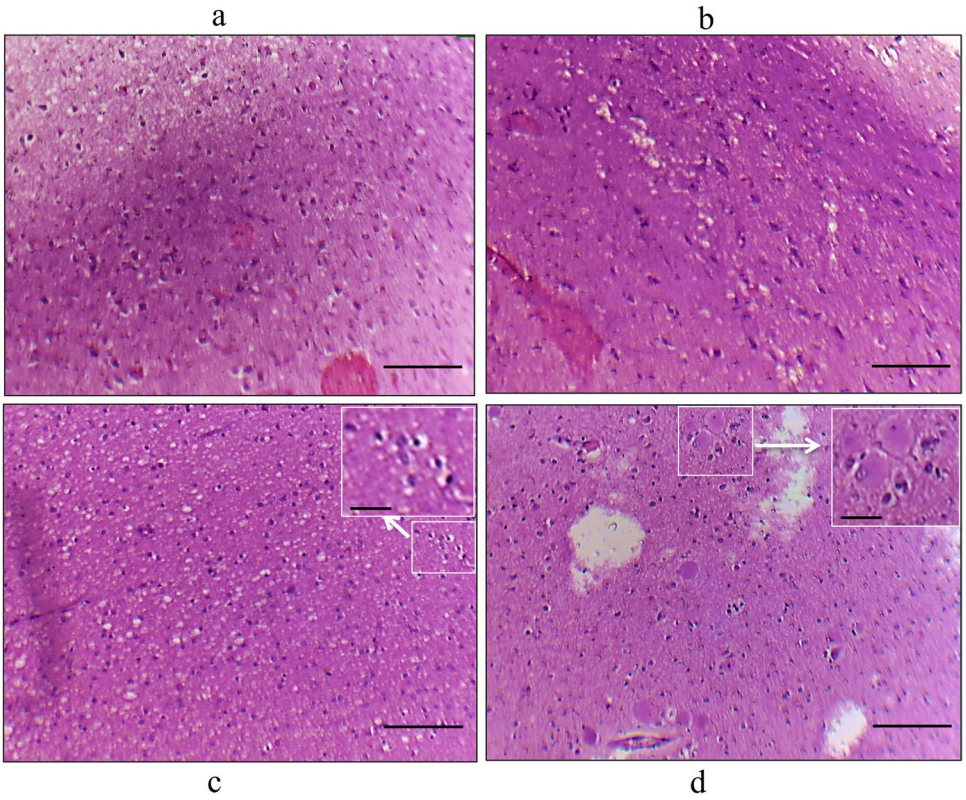

Fig. 1 Histopathology of FCD types. histopathology of FCD type I and type II: Image was taken using the Olympus microscope. Hematoxylin and eosin staining showed abnormal cortical architecture in FCDI: (**a**) dyslamination and disorganization in the cortex, **b** columnar disorganization in the cortex, **c** FCD IIa showing dysmorphic neurons, and **d** FCD IIb dysmorphic neurons and balloon cells having large cytoplasm with single or multi nuclei. The scale bar for Fig. 1 a, b, c, and d is 100 µm, and for the high magnification inserts (Fig. 1c, d in white box) 30 µm

and Blower 2016). Thioflavin T assay (ThT) was performed to determine the fluorescent intensity of accumulated unfolded protein aggregates in ($n=26$) patient samples (Fig. 2). The ThT assay showed a significant difference in fluorescence intensity of UFP aggregates in class 3 patients ($P<0.001$, 367.15 ± 4.85) compared to class 2 ($P<0.31$, 280.02 ± 3.36) and class 1 ($P<0.004$, 219.63 ± 3.64).

ER stress response in FCD patients

The correlation between ThT and post-surgical clinical data suggests that patients who showed complete seizure outcomes had reduced accumulation of UFP and vice versa. We have performed the western blot analysis by selecting $n=3$ samples from each ILAE class to understand the molecular changes associated with protein folding and protein degradation signaling mechanisms. The patient samples found no significant change or close variation while performing UFP detection assays were pooled and taken as one sample. Figure 3a represents the western blot assay for ER stress response signals against the accumulation of unfolded proteins by activating protein degradation machinery. All FCD patient samples belonging to ILAE classes 1, 2, and 3 showed a significant increase ($P<0.001$, 2.35 ± 0.12, 2.59 ± 0.24, 2.63 ± 0.23) in the staining intensity of BiP/GRP78 (Fig. 3b). The ER transmembrane receptor pIRE1α protein (Fig. 3c) staining intensity showed a significant increase in class 3 ($P<0.001$, 2.59 ± 0.18) than class 2 ($P<0.02$, 1.87 ± 0.16) but not with class 1 (2.15 ± 0.39). The downstream target of pIRE1α is XBP1. We have measured the XBP1 spliced (active) forms using western blot analysis (Fig. 3d) and immunofluorescence assay (Fig. 4). The XBP1s (s-spliced) form staining intensity was significantly increased in ILAE classes 1 and 3 ($P<0.003$, 1.29 ± 0.10; $P<0.003$, 1.35 ± 0.13) respectively, compared to class 2 ($P<0.03$, 0.90 ± 0.09), and immunofluorescence assay reconfirms the upregulation of XBP1s through increased fluorescence intensity in ILAE classes 1 and 3 ($P<0.002$, 3.15 ± 0.25; $P<0.003$, 3.25 ± 0.23), respectively, compared to class 2 ($P<0.04$, 1.69 ± 0.24). The p-IRE1-XBP1 axis can further activate ER-associated protein degradation machinery and chaperones, i.e., BiP, to increase the protein folding capacity to ameliorate unfolded protein response (UPR) by ER. In our study, we observed significant increase in peIF2α (Fig. 3e) staining intensity in ILAE class 3 ($P<0.002$, 2.86 ± 0.33) compared to class 1 ($P<0.006$, 1.26 ± 0.25), and class 2 ($P<0.008$, 1.57 ± 0.29), respectively. The above data suggest reduced protein aggregates and the absence of translational attenuation in ILAE class 1 patient samples and the occurrence of severe ER stress due to the accumulation of unfolded proteins in ILAE class 2 and 3 patient samples.

Table 1 Clinical data of the study population representing seizure-free outcome according to ILAE classification. Class 1 = 38.46% (complete seizure-free, no auras), Class 2 = 34.61% (only auras and < 1 seizures per year), and Class 3 = 26.92% (< 3 seizures per year and auras). The controls are obtained from NIMHANS, Bangalore

S. no	Gender	FCD type	Age of onset	Surgery age	Epilepsy duration	Location of FCD	ILAE outcome classification
1	Male	FCDI	12 years	40 years	28 years	Frontal	Class 2
2	Male	FCDI	11 years	13 years	2 years	Parietal	Class 1
3	Male	FCDI	3 years	15 years	12 years	Parietal	Class 2
4	Female	FCDIIb	6 months	4.6 years	4 years	Frontal	Class 1
5	Female	FCDI	16 years	27 years	11 years	Frontal	Class 1
6	Male	FCDIIa	10 years	13 years	3 years	Frontal	Class 3
7	Female	FCDIIb	14 months	12 years	10 years 10 months	Frontal	Class 1
8	Male	FCDI	8 years	12 years	4 years	Occipital	Class 2
9	Female	FCDI	6 years	14 years	8 years	Frontal	Class 2
10	Female	FCDI	5 years	18 years	13 years	Frontal	Class 3
11	Male	FCDI	9.5 years	10 years	7 months	Frontal	Class 3
12	Female	FCDIIa	2 years	14 years	12 years	Frontal	Class 2
13	Male	FCDIIb	5 years	8 years	3 years	Frontal	Class 1
14	Male	FCDI	34 years	35 years	1 year	Frontal	Class 2
15	Male	FCDIIa	2 years	25 years	23 years	Frontal	Class 1
16	Male	FCDIIb	11 years	21 years	10 years	Frontal	Class 1
17	Male	FCDI	6 years	13 years	7 years	Parietal	Class 3
18	Female	FCDIIb	3 years	3 years	2 years	Frontal	Class 1
19	Male	FCDIIa	11 years	14 years	3 years	Frontal	Class 3
20	Male	FCDIIb	15 years	25 years	10 years	Frontal	Class 2
21	Male	FCDI	1 year	11 years	10 years	Occipital	Class 3
22	Male	FCDI	4 years	10 years	6 years	Frontal	Class 3
23	Female	FCDIIb	2 years	4 years	2 years	Frontal	Class 1
24	Female	FCDIIb	2 years	15 years	13 years	Frontal	Class 1
25	Male	FCDI	12 years	25 years	13 years	Frontal	Class 2
26	Male	FCDI	13 years	27 years	14 years	Frontal	Class 2

Table 2 Control case information: The controls are obtained from NIMHANS, Bangalore. Storage and sample processing were performed by NIMHANS, human brain tissue repository, according to their standardized protocol to use the brain tissue for the research purpose

S. no	Gender	Age	Cause of death	Post-mortem interval	Significant neuropathology	Disease	HIV/HBsAg	Brain region
1	Male	19 years	Drowning	30 h	Cerebral injury	No	Negative	Frontal
2	Male	25 years	Homicide	25 h	Absent	No	Negative	Parietal
3	Female	35 years	Heart attack	35 h	Absent	Diabetes	Negative	Occipital

ER-induced autophagy response may not be sufficient to clear protein aggregates

The Beclin 1 (Fig. 5b) staining intensity was significantly higher in ILAE class 1 ($P < 0.01$, 1.09 ± 0.10) class 2 ($P < 0.009$, 1.29 ± 0.12), and class 3 ($P < 0.05$, 1.24 ± 0.10). Upregulation of Beclin 1 suggests how critical the autophagy signal is for classes 1, 2, and 3 to clear the aggregated proteins. Furthermore, the staining intensity of ATG7 (Fig. 5c) increased in class 3 ($P < 0.001$, 14.02 ± 3.23) than the ILAE 2 ($P < 0.03$, 7.81 ± 2.02) and ILAE 1 ($P < 0.02$, 7.94 ± 1.51), ATG12-5 (Fig. 5d) significantly increased in class 2 ($P < 0.003$, 2.21 ± 0.1) and class 3 ($P < 0.002$, 2.56 ± 0.39) than class 1 ($P < 0.05$, 1.07 ± 0.051), and ATG16L1 (Fig. 5e) significantly higher in class 3 ($P < 0.001$, 76.88 ± 5.57) than class 2 ($P < 0.03$, 45.92 ± 11.59) and class 1 ($P < 0.02$, 37.12 ± 6.34). Sequsetosome1/p62 (Fig. 5f), a critical

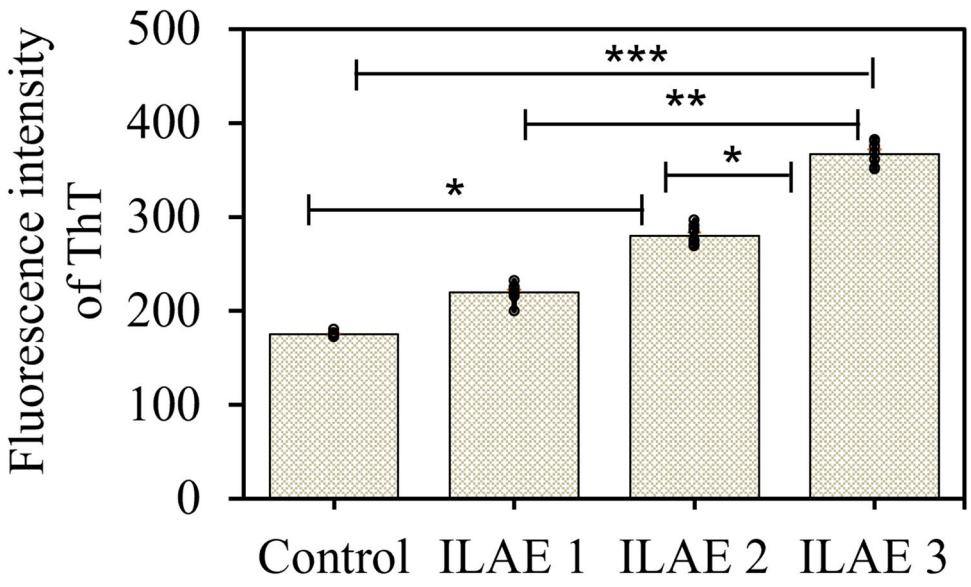

Fig. 2 Estimation of protein aggregates by ThT assay: ThT assay was performed to understand the unfolded protein aggregates in FCD patient samples ($n=26$). The fluorescence intensity of ThT bound to protein aggregates was measured and shown as mean ± SEM. These results are representative of 3 independent experiments. Thioflavin T assay for focal cortical dysplasia (FCD) samples was performed based on clinical parameters; class 3 ($P<0.001$) and class 2 ($P<0.03$) showed a significant increase compared to ILAE class 1

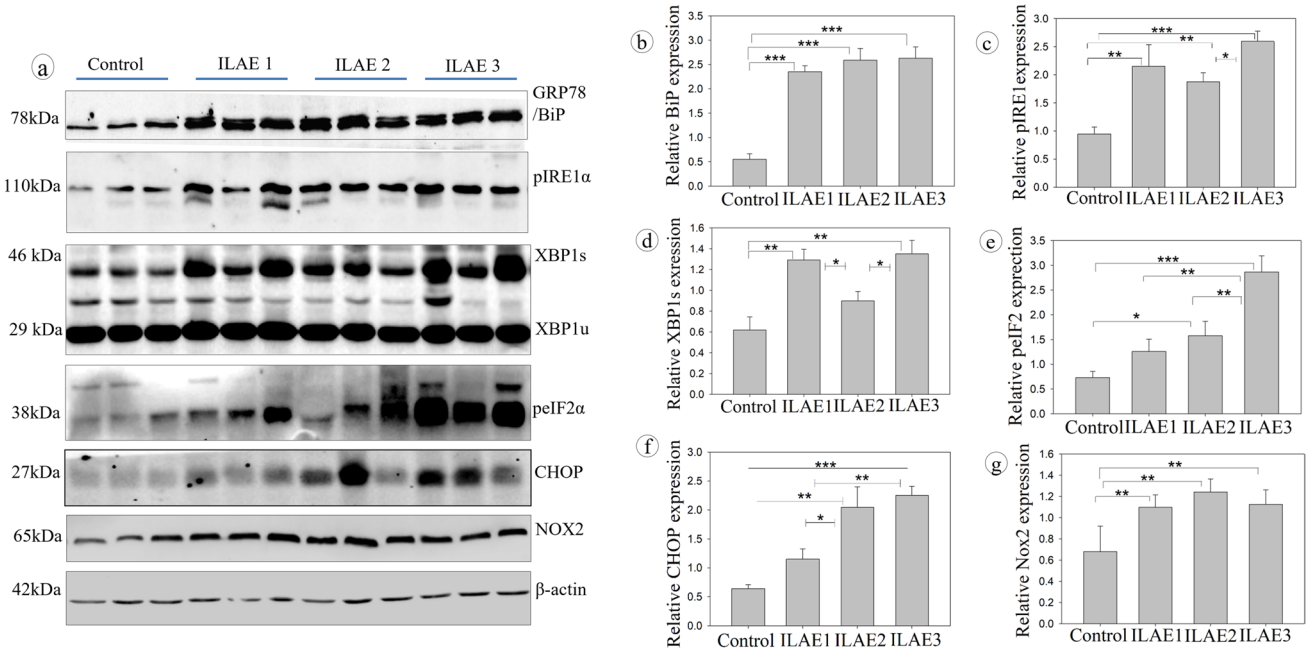

Fig. 3 Western blot analysis of ER stress response in FCD patient samples: Immunoblot assay for ER stress: Bip/GRP78, p-IRE1α, XBP1, p-eIF2 α, CHOP, NOX2, and β-actin in control and epileptic patient resected brain samples. An equal amount of protein was loaded in SDS-PAGE and transferred onto NC membranes, then blocked with nonfat milk and probed with primary antibody. The lane represents the control and FCD ($n=3$). The band/signal intensity was quantified (Relative protein expression) and shown as mean ± SEM. Densitometry analysis (**b**–**g**) showed a significant increase in BiP/GRP78, p-IRE1α, XBP1, p-eIF2 α, CHOP, and Nox2 in the FCD samples belonging to ILAE classes 2 and 3 than class 1 and controls. *$P<0.05$, **$P<0.01$, ***$P<0.001$

autophagy cargo protein's staining intensity, was found to be increased in ILAE classes 2 ($P<0.01$, 3.61 ± 0.52) and class 3 ($P<0.001$, 4.84 ± 0.27) significantly than class 1 ($P<0.04$, 1.76 ± 0.55); since p62 is degraded along with autophagy proteins, its abundance infers impaired autophagy. The LC3B type II (Fig. 5g) staining intensity was significantly higher in ILAE class 3 ($P<0.001$, 10.17 ± 1.27) than in class 1 ($P<0.005$, 4.74 ± 1.53). At the same time, class 2 ($P<0.01$, 7.61 ± 0.65) showed a significant increase compared to class 1 (4.74 ± 1.53). Since LC3B II and p62 themselves undergo autophagy degradation (González-Rodríguez et al. 2014), their abundance/accumulation is a good sign of impaired autophagy and increased ER stress in ILAE class 2 and class 3 patients.

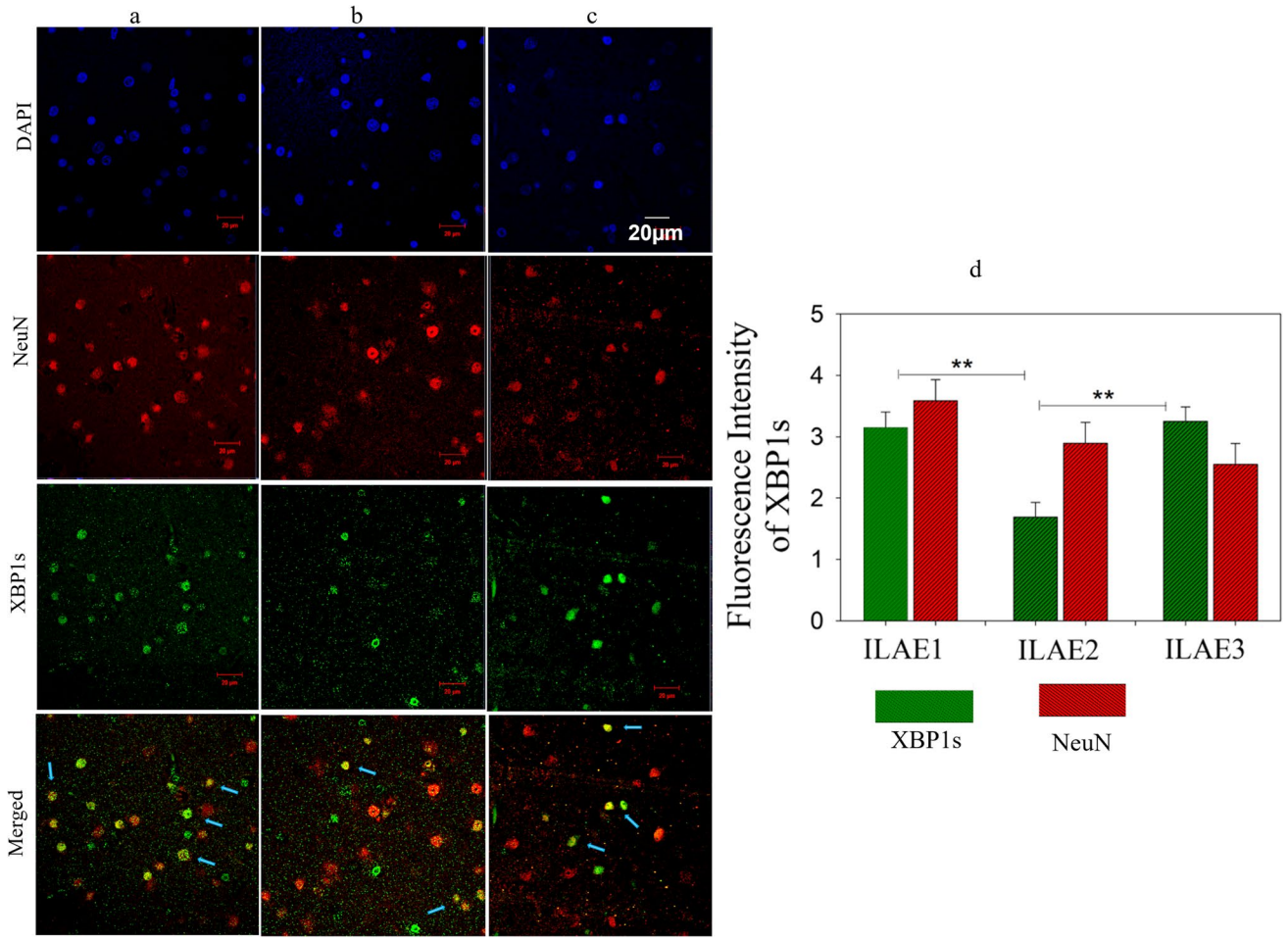

Fig. 4 Double immunofluorescence study for XBP1 expression in FCD (colored image). Double immunofluorescence assay. Staining of XBP1s (green) and NeuN (red) **a**, **b**, and **c** represents the neuronal expression of XBP1s in ILAE outcome classes 1, 2, and 3 of FCD patient's brain sections ($n=3$), respectively. The blue color represents di-amidino phenylindole (DAPI) staining used as a nuclear counterstain. The arrowheads in the merged image of NeuN + XBP1s represent the localization of XBP1s in neuronal cells. The fluorescence intensity of XBP1s was quantified and shown as mean ± SEM. Class 1 (**a**) > Class 2 (**b**) < Class 3 (**c**). Scale bar = 20 µm. Data is representative of 3 independent experiments

Chronic ER stress response inducing apoptosis

ER stress response initiates autophagy signaling to clear the UFP aggregates during stress conditions. In some chronic stress conditions, the cells may fail to eliminate excess proteins due to factors that inhibit or overthrow the autophagy machinery and lead to the activation of the apoptosis signal. In FCD patients, Nox2 (Fig. 3g), protein staining intensity was increased in class 1 ($P<0.01$, 1.09 ± 0.12) class 2 ($P<0.007$, 1.13 ± 0.12), and 3 ($P<0.009$, 1.12 ± 0.13); this suggests the ROS accumulation in patient samples. Nox2 increases the synthesis of ROS and also disturbs the autophagy mechanism. In addition, we have observed a significant increase in CHOP protein staining intensity through western blot assay in class 2 ($P<0.009$, 2.05 ± 0.35) and class 3 ($P<0.001$, 2.25 ± 0.16) compared to the ILAE class 1 ($P<0.02$, 1.15 ± 0.18) patients (Fig. 3f). CHOP acts as an apoptosis initiation factor during impaired autophagy and severe ER stress. All the FCD samples belonging to ILAE classes 1, 2, and 3 were found to have a significant increase in UPR and autophagy signaling proteins and UFP aggregates compared to control brain samples.

Discussion

One-third of patients who have epilepsy show poor responses to current anti-epileptic drugs (Liu et al. 2019) and require the surgical resection of epileptic foci. Many patients benefit from epilepsy surgery, but still, some are vulnerable to seizure recurrence (Goodman 2011). During epilepsy, excitotoxicity disturbs cellular functions such as protein folding

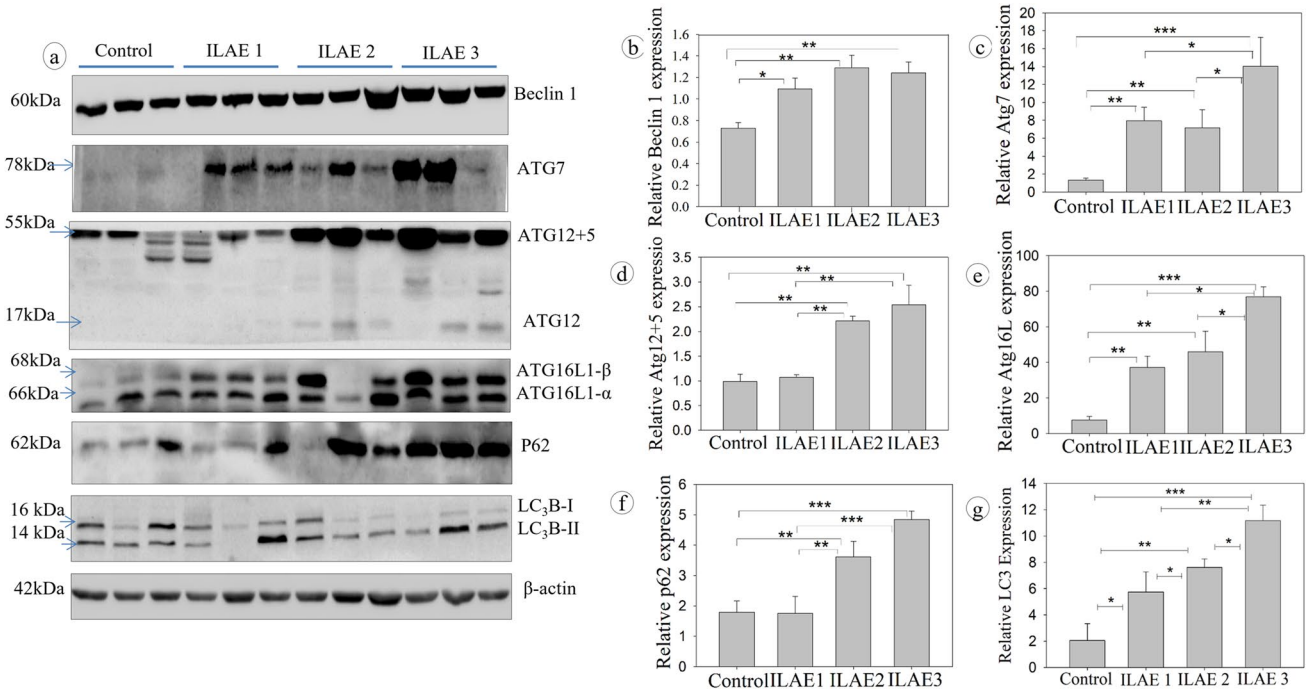

Fig. 5 Western blot analysis of autophagy response in FCD patient samples: Immunoblot assay for autophagy: Beclin, ATG7, ATG12-5, ATG16L1, p62, LC3B, and β-actin in control and epileptic patient resected brain samples. An equal amount of protein was loaded in SDS-PAGE, transferred onto NC membranes, blocked with nonfat milk, and then probed with a primary antibody. The lanes represent the control and FCD samples. The band/signal intensity was quantified (relative protein expression) and shown as mean ± SEM. Densitometry analysis (**b**–**g**) shows a significant increase in Beclin1, ATG7, ATG12 + 5, ATG16L1, P62, and LC3B in the FCD samples belonging to ILAE classes 2 and 3 than class 1 and controls ($n = 3$). *$P < 0.05$, **$P < 0.01$, ***$P < 0.001$

and sorting (Liu et al., 2019) also free radicle production (Frantseva et al. 2000), but the severity and duration vary among individuals. These events disturb the ER homeostasis and lead to the activation of stress response signals to maintain cellular homeostasis by attenuating new protein synthesis and clearing the UFP aggregates. Since patients exhibit different cellular and molecular changes during seizures, the epileptic brain tissue resected during surgery is archetypal to understanding epileptogenesis (Dixit et al. 2017). This study aimed to find the UPR and autophagy changes that occurred in the FCD patients using resected epileptic brain samples to understand the possibility of a relation between ER stress and clinical outcomes in FCD patients.

Thioflavin T assay indicates the accumulation of UFP in FCD patients. Irrespective of age, gender, seizure foci, and severity, some patients had limited UFP, whereas few did not. Since we have observed the post-surgical follow-up data regularly to understand the clinical outcomes, we have categorized the patient cohort ($n = 26$) according to ILAE suggested outcome classes (Wieser et al. 2001): the ILAE class 1 (seizures-free), class 2 (< 1 seizure episode/year and auras), and class 3 (two to three seizure episodes/year and auras). Our findings showed the correlation between seizure outcomes and UFP aggregates. Patients with limited UFP levels suggest possible re-establishment of ER homeostasis, whereas increased UFP represents the possibility of repeated acute or chronic ER stress with auras and seizure recurrence. We believe that understanding the role of ER stress significance can help us to predict the possibility of seizure recurrence.

Based on these observations, we further studied the expression pattern of UPR and autophagy signaling proteins. We began with GRP78/BiP protein expression; BiP is an ER lumen resident chaperone that helps in the proper folding of nascent/unfolded proteins (Urano et al. 2000). Since UFP aggregates increased in patients, we have observed significant upregulation of BiP in all the patient samples which could help in the protein folding. In epilepsy, activation of IRE1α (pSer723) is a sign of ER stress UPR response (Liu et al. 2011, 2013; Feldman et al. 2016). IRE1α is inactive as long as BiP is bound to it; the presence of UFP in epilepsy patients released the BiP, which allowed the autophosphorylation and activation of IRE1α. Activated IRE1α (pSer724) splices XBP1 mRNA into XBP1s (Sidrauski and Walter 1997; Yoshida et al. 2001; Wang et al. 2012). During the accumulation of UFP, cells can adapt to acute (last for a few minutes to hours) or chronic ER stress responses (a few days to years) to retain the ER homeostasis (Liu et al. 2019). The

increased expression of XBP1s is a possible sign of chronic ER stress in ILAE classes 1 and 3, and we assume the possibility of adaptive chronic ER stress in ILAE class 1 compared to class 3. Similarly, class 2 patients probably adapted acute ER stress, which lasts for a while and helps to reduce the UFP aggregates. Therefore, adaptation to acute ER stress response could be one of the reasons for reduced XBP1 expression in class 2 patient samples. The acute-repetitive and chronic non-adaptive ER stress responses can worsen seizures in epilepsy patients by reducing the seizure threshold (Eggers 2007a, b; Liu and Connor 2015). Studies on human and mouse models showed significant upregulation of peIF2α (Ser51) during status epilepticus and hippocampal sclerosis (Petrov et al. 2003; Carnevalli et al. 2004), which represents the attenuation of global protein synthesis due to the inability of cells to limit the UFP in the ER (Boyce et al. 2005). The expression pattern of GRP78/BiP, pIRE1α, XBP1s, peIF2α, and ThT assay results suggest that ILAE class 1 patients readily get rid of UFP aggregates compared to ILAE classes 2 and 3.

ER stress response can control both autophagy and apoptosis signals depending on the severity of ER stress (Nishitoh 2002; Liu et al. 2011, 2013; Margariti et al. 2013; Jiang et al. 2015). In our study, we observed a significant increase in the expression of Beclin1 protein in all the FCD patient samples. Growing evidence also supports the relationship between impaired autophagy and epilepsy (Wong 2013; Lv and Ma 2020). Hence, we further elucidate the difference in autophagy signaling among the ILAE outcome classes. Autophagy response proteins (ATGs) are recruited to the ER and autophagy membrane upon autophagy induction (Nishimura and Tooze 2020). Since ATG 7 increases autophagy and reduces ER stress (Zheng et al. 2019), class 1 samples showed ATG7 upregulation but not class 2, which suggests impaired autophagy. Atg16L is a part of the core autophagy protein associated with the Atg12-5 complex (Kuma et al. 2002), which was increased in ILAE classes 2 and 3 patients. P62/SQSTM1 is an autophagy adaptor protein that degrades in the autophagosome (Pankiv et al. 2007). In our patient cohort, samples belonging to ILAE classes 2 and 3 showed the accumulation of p62 protein and LC3B, suggesting the possibility of impaired autophagy because of chronic ER stress (González-Rodríguez et al. 2014).

FCD patients were found to have increased NADPH oxidase 2 expression. Nox2 increases ROS formation, which could induce chronic ER stress, alter autophagy, even cause cell death, and contribute to increased seizure susceptibility (Bedard and Krause 2007; Pal et al. 2016; Huang et al. 2018; Fan et al. 2019). Increased Nox2, peIF2α, UFP, p62, and LC3B suggest the possibility of dysregulated chronic ER stress that can disturb the UPR and autophagy. CHOP has a dual role, which acts as an autophagy or apoptosis inducer (B'chir et al. 2014). Several studies have reported that during severe ER stress, CHOP acts as a pro-apoptotic molecule and promotes cell death (Szegezdi et al. 2006; Kim et al. 2008), which can create hyperexcitable seizure-sensitive cellular circuits (Wong 2013). Our findings were in line with the above statement.

Conclusion

The epileptic patients, who are seizure-free, were found to have reduced protein aggregates. On the other hand, patients with seizure recurrence had increased UFP aggregates due to disturbed ER homeostasis. This study explained how the brain's protection mechanism deals with seizures. We believe further studies about ER stress and epilepsy using more clinical samples and animal models can help consolidate our findings about epilepsy progression and clinical outcomes.

Supplementary Information The online version contains supplementary material available at https://doi.org/10.1007/s12192-022-01301-0.

Acknowledgements Human Brain Tissue Repository for Neurobiological Studies, Department of Neuropathology, National Institute of Mental Health and Neurosciences, Bangalore, India, provided the autopsied control brain samples for this study. We thank Dr. Sailaja (Department of Pathology, Krishna Institute of Medical Science, Secunderabad, India) for technical assistance with data collection.

Funding The study received financial assistance to the lab from the Ministry of Science and Technology, Department of Science and Technology, Government of India, DST-SERB Core grant, file no. CRG/2020/005021, DST-CSRI file nos. SR/CSRI/196/2016 and CRG/2020/005021; Department of Biotechnology, Government of India, BT/PR18168/MED/29/1064/2016, BT/PR17686/MED/30/1664/2016; and financial support to the University of Hyderabad-IoE by the Ministry of Education, Government of India (F11/9/2019-U3 (A), DST-FIST and UGC-SAP for the department. Kishore Madamanchi also received CSIR-UGC Fellowship (Ref. no: 22/12/2013(II) EU-V (341059)).

Declarations

Disclaimer The funding body had no role in the design, collection of the sample, management, the conduct of the study, interpretation of data, preparation, review, or approval of the manuscript, or decision to submit the manuscript for publication.

Conflict of interest The authors declare no competing interests.

Limitations Postoperative seizure outcome can be determined by multiple clinical factors, including the onset of epilepsy, multiple seizure semiologies, preoperative psychiatric comorbidities, type of dysplasia, and complete resection of the lesion. Individually comparing each factor with tissue ER stress could be challenging in such a limited sample.

References

B'chir W, Chaveroux C, Carraro V et al (2014) Dual role for CHOP in the crosstalk between autophagy and apoptosis to determine cell fate in response to amino acid deprivation. Cell Signal 26:1385–1391. https://doi.org/10.1016/j.cellsig.2014.03.009

B'chir W, Maurin A-C, Carraro V et al (2013) The eIF2α/ATF4 pathway is essential for stress-induced autophagy gene expression. Nucleic Acids Res 41:7683–7699. https://doi.org/10.1093/nar/gkt563

Bedard K, Krause K-H (2007) The NOX family of ROS-generating NADPH oxidases: physiology and pathophysiology. Physiol Rev 87:245–313. https://doi.org/10.1152/physrev.00044.2005

Beriault DR, Werstuck GH (2013) Detection and quantification of endoplasmic reticulum stress in living cells using the fluorescent compound, Thioflavin T. Biochimica et Biophysica Acta (BBA) - Mol Cell Res 1833:2293–2301. https://doi.org/10.1016/j.bbamcr.2013.05.020

Boyce M, Bryant KF, Jousse C et al (2005) A selective inhibitor of eIF2α dephosphorylation protects cells from ER stress. Science 307:935–939. https://doi.org/10.1126/science.1101902

Bravo R, Parra V, Gatica D et al (2013) Endoplasmic reticulum and the unfolded protein response. Int Rev Cell Mol Biol 215–290. https://doi.org/10.1016/B978-0-12-407704-1.00005-1

Carnevalli LS, Pereira CM, Longo BM et al (2004) Phosphorylation of translation initiation factor eIF2α in the brain during pilocarpine-induced status epilepticus in mice. Neurosci Lett 357:191–194. https://doi.org/10.1016/j.neulet.2003.12.093

Dixit AB, Banerjee J, Tripathi M et al (2017) Synaptic roles of cyclin-dependent kinase 5 & its implications in epilepsy. Indian J Med Res 145:179–188. https://doi.org/10.4103/ijmr.IJMR_1249_14

Eggers AE (2007a) Redrawing Papez' circuit: A theory about how acute stress becomes chronic and causes disease. Med Hypotheses 69:852–857. https://doi.org/10.1016/j.mehy.2007.01.074

Eggers AE (2007b) Temporal lobe epilepsy is a disease of faulty neuronal resonators rather than oscillators, and all seizures are provoked, usually by stress. Med Hypotheses 69:1284–1289. https://doi.org/10.1016/j.mehy.2007.03.025

Fan LM, Geng L, Cahill-Smith S et al (2019) Nox2 contributes to age-related oxidative damage to neurons and the cerebral vasculature. J Clin Investig 129:3374–3386. https://doi.org/10.1172/JCI125173

Feldman HC, Tong M, Wang L et al (2016) Structural and functional analysis of the allosteric inhibition of IRE1α with ATP-competitive ligands. ACS Chem Biol 11:2195–2205. https://doi.org/10.1021/acschembio.5b00940

Frantseva MV, Velazquez JLP, Hwang PA, Carlen PL (2000) Free radical production correlates with cell death in an in vitro model of epilepsy. Eur J Neurosci 12:1431–1439. https://doi.org/10.1046/j.1460-9568.2000.00016.x

González-Rodríguez Á, Mayoral R, Agra N et al (2014) Impaired autophagic flux is associated with increased endoplasmic reticulum stress during the development of NAFLD. Cell Death Dis 5:e1179–e1179. https://doi.org/10.1038/cddis.2014.162

Goodman RR (2011) AES 2009 annual course: reoperation for medically refractory epilepsy. Epilepsy Behav 20:241–246. https://doi.org/10.1016/j.yebeh.2010.12.025

Harding HP, Zhang Y, Ron D (1999) Protein translation and folding are coupled by an endoplasmic-reticulum-resident kinase. Nature 397:271–274. https://doi.org/10.1038/16729

Henríquez-Olguin C, Knudsen JR, Raun SH et al (2019) Cytosolic ROS production by NADPH oxidase 2 regulates muscle glucose uptake during exercise. Nat Commun 10:4623. https://doi.org/10.1038/s41467-019-12523-9

Hu H, Tian M, Ding C, Yu S (2019) The C/EBP homologous protein (CHOP) transcription factor functions in endoplasmic reticulum stress-induced apoptosis and microbial infection. Front Immunol 9. https://doi.org/10.3389/fimmu.2018.03083

Huang W-Y, Lin S, Chen H-Y et al (2018) NADPH oxidases as potential pharmacological targets against increased seizure susceptibility after systemic inflammation. J Neuroinflammation 15:140. https://doi.org/10.1186/s12974-018-1186-5

Jiang D, Niwa M, Koong AC (2015) Targeting the IRE1α–XBP1 branch of the unfolded protein response in human diseases. Semin Cancer Biol 33:48–56. https://doi.org/10.1016/j.semcancer.2015.04.010

Kabat J, Król P (2012) Ogniskowa dysplazja korowa – stan obecny wiedzy. Pol J Radiol 77:35–43. https://doi.org/10.12659/PJR.882968

Kadowaki H, Nishitoh H (2013) Signaling pathways from the endoplasmic reticulum and their roles in disease. Genes (basel) 4:306–333. https://doi.org/10.3390/genes4030306

Kim I, Xu W, Reed JC (2008) Cell death and endoplasmic reticulum stress: disease relevance and therapeutic opportunities. Nat Rev Drug Discov 7:1013–1030. https://doi.org/10.1038/nrd2755

Kim SH, Choi J (2019) Pathological classification of focal cortical dysplasia (FCD): personal comments for well understanding FCD classification. J Korean Neurosurg Soc 62:288–295. https://doi.org/10.3340/jkns.2019.0025

Krsek P, Maton B, Korman B et al (2008) Different features of histopathological subtypes of pediatric focal cortical dysplasia. Ann Neurol 63:758–769. https://doi.org/10.1002/ana.21398

Kuma A, Mizushima N, Ishihara N, Ohsumi Y (2002) Formation of the ~350-kDa Apg12-Apg5·Apg16 multimeric complex, mediated by Apg16 oligomerization, is essential for autophagy in yeast. J Biol Chem 277:18619–18625. https://doi.org/10.1074/jbc.M111889200

Kwan P, Arzimanoglou A, Berg AT et al (2010) Definition of drug resistant epilepsy: consensus proposal by the ad hoc task force of the ILAE Commission on therapeutic strategies. Epilepsia 51:1069–1077. https://doi.org/10.1111/j.1528-1167.2009.02397.x

Liu D-C, Eagleman DE, Tsai N-P (2019) Novel roles of ER stress in repressing neural activity and seizures through Mdm2- and p53-dependent protein translation. PLoS Genet 15:e1008364. https://doi.org/10.1371/journal.pgen.1008364

Liu G, Guo H, Guo C et al (2011) Involvement of IRE1α signaling in the hippocampus in patients with mesial temporal lobe epilepsy. Brain Res Bull 84:94–102. https://doi.org/10.1016/j.brainresbull.2010.10.004

Liu G-L, Wang K-Y, Guo H et al (2013) Inositol-requiring protein 1α signaling pathway is activated in the temporal cortex of patients with mesial temporal lobe epilepsy. Neurol Sci 34:357–364. https://doi.org/10.1007/s10072-012-1008-y

Liu Y, Connor J (2015) From adaption to death: endoplasmic reticulum stress as a novel target of selective neurodegeneration? Neural Regen Res 10:1397. https://doi.org/10.4103/1673-5374.165227

Lv M, Ma Q (2020) Autophagy and Epilepsy. Adv Exp Med Biol 163–169. https://doi.org/10.1007/978-981-15-4272-5_10

Margariti A, Li H, Chen T et al (2013) XBP1 mRNA splicing triggers an autophagic response in endothelial cells through BECLIN-1 transcriptional activation. J Biol Chem 288:859–872. https://doi.org/10.1074/jbc.M112.412783

Nishimura T, Tooze SA (2020) Emerging roles of ATG proteins and membrane lipids in autophagosome formation. Cell Discov 6:32. https://doi.org/10.1038/s41421-020-0161-3

Nishitoh H (2002) ASK1 is essential for endoplasmic reticulum stress-induced neuronal cell death triggered by expanded polyglutamine repeats. Genes Dev 16:1345–1355. https://doi.org/10.1101/gad.992302

Oyadomari S, Koizumi A, Takeda K et al (2002) Targeted disruption of the Chop gene delays endoplasmic reticulum stress–mediated diabetes. J Clin Investig 109:525–532. https://doi.org/10.1172/JCI14550

Oyadomari S, Mori M (2004) Roles of CHOP/GADD153 in endoplasmic reticulum stress. Cell Death Differ 11:381–389. https://doi.org/10.1038/sj.cdd.4401373

Pal R, Bajaj L, Sharma J et al (2016) NADPH oxidase promotes Parkinsonian phenotypes by impairing autophagic flux in an mTORC1-independent fashion in a cellular model of Parkinson's disease. Sci Rep 6:22866. https://doi.org/10.1038/srep22866

Pal R, Palmieri M, Loehr JA et al (2014) Src-dependent impairment of autophagy by oxidative stress in a mouse model of Duchenne muscular dystrophy. Nat Commun 5:4425. https://doi.org/10.1038/ncomms5425

Palmini A, Najm I, Avanzini G et al (2004) Terminology and classification of the cortical dysplasias. Neurology 62:S2–S8. https://doi.org/10.1212/01.WNL.0000114507.30388.7E

Pankiv S, Clausen TH, Lamark T et al (2007) p62/SQSTM1 binds directly to Atg8/LC3 to facilitate degradation of ubiquitinated protein aggregates by autophagy. J Biol Chem 282:24131–24145. https://doi.org/10.1074/jbc.M702824200

Petrov T, Rafols JA, Alousi SS et al (2003) Cellular compartmentalization of phosphorylated eIF2α and neuronal NOS in human temporal lobe epilepsy with hippocampal sclerosis. J Neurol Sci 209:31–39. https://doi.org/10.1016/S0022-510X(02)00461-6

Rao RV, Ellerby HM, Bredesen DE (2004) Coupling endoplasmic reticulum stress to the cell death program. Cell Death Differ 11:372–380. https://doi.org/10.1038/sj.cdd.4401378

Schubert U, Antón LC, Gibbs J et al (2000) Rapid degradation of a large fraction of newly synthesized proteins by proteasomes. Nature 404:770–774. https://doi.org/10.1038/35008096

Schwarz DS, Blower MD (2016) The endoplasmic reticulum: structure, function and response to cellular signaling. Cell Mol Life Sci 73:79–94. https://doi.org/10.1007/s00018-015-2052-6

Sidrauski C, Walter P (1997) The Transmembrane Kinase Ire1p Is a Site-Specific Endonuclease That Initiates mRNA Splicing in the Unfolded Protein Response. Cell 90:1031–1039. https://doi.org/10.1016/S0092-8674(00)80369-4

Sokka A-L, Putkonen N, Mudo G et al (2007) Endoplasmic reticulum stress inhibition protects against excitotoxic neuronal injury in the rat brain. J Neurosci 27:901–908. https://doi.org/10.1523/JNEUROSCI.4289-06.2007

Szegezdi E, Logue SE, Gorman AM, Samali A (2006) Mediators of endoplasmic reticulum stress-induced apoptosis. EMBO Rep 7:880–885. https://doi.org/10.1038/sj.embor.7400779

Urano F, Bertolotti A, Ron D (2000) IRE1 and efferent signaling from the endoplasmic reticulum. J Cell Sci 113:3697–3702. https://doi.org/10.1242/jcs.113.21.3697

Wang L, Perera BGK, Hari SB et al (2012) Divergent allosteric control of the IRE1α endoribonuclease using kinase inhibitors. Nat Chem Biol 8:982–989. https://doi.org/10.1038/nchembio.1094

Wieser HG, Blume WT, Fish D et al (2001) ILAE Commission Report. Proposal for a new classification of outcome with respect to epileptic seizures following epilepsy surgery. Epilepsia 42:282–286

Wong M (2013) Cleaning up epilepsy and neurodegeneration: the role of autophagy in epileptogenesis. Epilepsy Curr 13:177–178. https://doi.org/10.5698/1535-7597-13.4.177

Wu J, Kaufman RJ (2006) From acute ER stress to physiological roles of the unfolded protein response. Cell Death Differ 13:374–384. https://doi.org/10.1038/sj.cdd.4401840

Yoshida H, Matsui T, Yamamoto A et al (2001) XBP1 mRNA is induced by ATF6 and spliced by IRE1 in response to ER stress to produce a highly active transcription factor. Cell 107:881–891. https://doi.org/10.1016/S0092-8674(01)00611-0

Zheng W, Xie W, Yin D et al (2019) ATG5 and ATG7 induced autophagy interplays with UPR via PERK signaling. Cell Communication and Signaling 17:42. https://doi.org/10.1186/s12964-019-0353-3

Zhu X, Dong J, Han B et al (2017) Neuronal nitric oxide synthase contributes to PTZ kindling epilepsy-induced hippocampal endoplasmic reticulum stress and oxidative damage. Front Cell Neurosci 11. https://doi.org/10.3389/fncel.2017.00377

Zinszner H, Kuroda M, Wang X et al (1998) CHOP is implicated in programmed cell death in response to impaired function of the endoplasmic reticulum. Genes Dev 12:982–995. https://doi.org/10.1101/gad.12.7.982